# Aerodynamic shape optimisation of hovering rotors using compressible CFD

**C. B. Allen**
**c.b.allen@bristol.ac.uk**
**T. C. S. Rendall**
**thomas.rendall@bristol.ac.uk**
Department of Aerospace Engineering
University of Bristol
Bristol, UK

## ABSTRACT

Generic wrap-around shape optimisation technology is presented, and is applied to a helicopter rotor in hover, using compressible CFD as the aerodynamic model. An efficient domain element shape parameterisation method is used as the surface control and deformation method, and is linked to a radial basis function global interpolation, to provide direct transfer of domain element movements into deformations of the design surface and the CFD volume mesh. This method is independent of mesh type and size, and optimisation independence from the flow solver is achieved by obtaining sensitivity information for an advanced parallel gradient-based algorithm by finite-difference. The method is applied here to a two-bladed hovering rotor, with transonic tip speed, comparing the effects of global twist parameters and more local planform parameters. Significant torque reductions are achieved in both cases, and it is shown that using only three global twist parameters are extremely effective. Using 63 local and global parameters, large geometric changes are demonstrated, with both induced power and wave drag reduced.

## NOMENCLATURE

| | |
|---|---|
| $c$ | aerofoil chord |
| $C_T$ | thrust coefficient |
| $C_Q$ | torque coefficient |
| $C_z$ | normal force coefficient |
| $C_{mx}, C_{my}, C_{mz}$ | hinge moment coefficients |
| M | Mach number |
| $N$ | number of interpolation control points |
| $p$ | polynomial term |
| $\mathbf{r}$ | co-ordinate vector |
| $s$ | interpolated function |
| $V$ | internal volume |
| $x,y,z$ | inertial co-ordinates |
| $\beta$ | interpolation coefficients |
| $\phi$ | basis function |
| $\sigma$ | rotor solidity |

### *Subscripts*

| | |
|---|---|
| $i$ | control point counter |

## 1.0 INTRODUCTION

Numerical simulation methods are now used routinely in industrial design, and increasing computer power has resulted in their increasing use in optimisation. Integrating an effective geometry control method with a flow-solver and a numerical optimisation scheme can result in an aerodynamic shape optimisation approach, and these are invaluable in the design stage. Furthermore, developing a modular approach means that the complexity and cost of each module required at various stages of the design process can be changed, in terms of aerodynamic fidelity, number of surface shape design degrees of freedom, and the complexity of the optimisation scheme.

**Paper No. 3608**. Manuscript received 5 July 2010, revised version received 26 November 2010, 2nd revised version received 26 March 2011, accepted 31 March 2011.
A version of this paper was first presented at The RAeS Aerodynamics Conference, Bristol, July 2010.

https://doi.org/10.1017/S0001924000006151 Published online by Cambridge University Press

Compressible CFD has been used in numerous optimisations of two-dimensional aerofoil sections[1,2], three-dimensional wings and aircraft[3-7], and aeroelastic aircraft[8,9], but little has been achieved in the way of rotors, primarily due to the high simulation cost. Higher density grids and longer solution integration times are required than for fixed-wing cases[10,11,12], and this can result in excessive computational power requirements to optimise such a system. There are also two distinct flow regimes, hover and forward flight, and good performance in one is unlikely to be carried over to the other. Aerodynamic optimisation has been applied previously to rotors in hover but mainly with both low fidelity aerodynamics and only gross geometric changes, see for example[13], with only a few notable results using compressible CFD, namely those of ONERA[14,15], Nadarajah *et al*[16], Choi *et al*[17], Nielsen *et al*[18], Imiela[19,20], and recent work of Johnson and Barakos[21,22]. The research presented here is aimed at the development of a modularised, generic optimisation tool, that is flow-solver and mesh type independent, and applicable to any aerodynamic problem; rotor blades in hover in this case.

A flexible optimisation and design process requires an effective geometry parameterisation process, that is flexible enough to allow sufficient design space investigation and robust enough to be applicable to any geometry or design surface. Furthermore, a small number of design parameters is desirable, particularly if using a finite-difference gradient evaluation. Related to the surface control is the required volume mesh deformation or regeneration once the design surface has been deformed, and mesh deformation is much preferred. To satisfy these requirements, an efficient combined domain element shape parameterisation and volume mesh deformation method has been developed by the authors, which is mesh type and size independent, and presented previously for CFD-based shape optimisation in two dimensions[23], three-dimensional fixed-wing optimisation[24], and initial rotor blade cases[25].

To ensure a modular framework and flow-solver independence, a finite-difference approach to parameter sensitivities has been adopted, and so a small number of design parameters is essential, which the domain element approach makes possible. This method has been coupled to an advanced gradient-based constrained optimisation algorithm, and the optimisation suite has been parallelised to allow optimisation of three-dimensional bodies in practical times.

Previous work[25] has applied the methods to hovering rotors using twist parameters only, to validate the approach. Minimum torque was the objective, with strict constraints on thrust, internal volume and pitching moments. The effects of global and local twist parameters were investigated, and significant torque reductions were achieved using only three global and 15 local twist parameters. Hence, this paper extends the parameterisation to allow more geometric flexibility, by using 63 local and global parameters, and results are compared to the global twist only results.

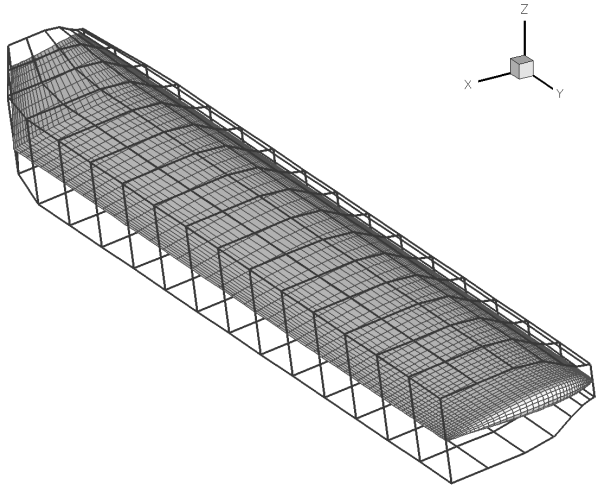



Figure 1. Initial rotor domain element and surface.

## 2.0 SURFACE PARAMETERISATION AND CONTROL

The problems of surface parameterisation and control during an optimisation process, and the required volume mesh deformation if using a CFD code, are often treated separately, but are treated simultaneously here. Shape parameterisation methods can be split into those that parameterise the aerodynamic mesh or those that parameterise the design geometry from which a mesh is generated. Mesh parameterisation methods are generally independent of the mesh generation package, and need to deform the initial mesh during an optimisation. Methods of this nature include discrete[26,27,28], analytical, basis vector[29], free form deformation (FFD)[30], domain element methods[31], and the control grid approach[32]. Geometry parameterisation methods are inherently linked with the mesh generation package, and optimisation requires automatic mesh generation tools. Methods of this nature include partial differential equation methods (PDE)[33], polynomial or spline[34], CAD and recently CST[35] methods. Reviews of a range of parameterisation methods are presented[36,37].

The mesh parameterisation approach has been adopted here, since this offers most flexibility, by allowing independence from both the mesh generation tools and the mesh structure. However, a mesh deformation scheme is required, and this is a significant issue. The efficient parameterisation method here links a set of aerodynamic mesh points to a domain element that controls the shape of the design surface. At the centre of this technique is a multivariate interpolation using radial basis functions, and this provides a direct mapping between the domain element, the surface geometry and the locations of grid points in the CFD volume mesh. This mapping is only required once for the initial design as the values of the parametric coordinates of the grid points with respect to the domain element remain constant throughout the optimisation, and updates to the geometry and the corresponding mesh are provided simultaneously by application of multivariate interpolation. This is extremely fast and efficient and results in very high quality mesh deformation, even for large deformations[38,39,40], and the approach is meshless, so requires no connectivity and is applicable to any mesh type. Domain element points and volume mesh points are simply treated as independent point clouds.

### 2.1 Interpolation formulation

Radial basis functions (RBFs) are a form of global interpolation function, that allow a global dependence to be evaluated between any point in n-dimensional space and a set of data points in the same space. The general theory of RBFs is presented in Refs 41 and 42, and the method used here is detailed in Refs 38 and 43. The solution of an interpolation problem using RBFs begins with the form of the required interpolation;

$$s(\mathbf{r}) = \sum_{i=1}^{i=N} \beta_i \phi_i (\| \mathbf{r} - \mathbf{r}_i \|) + p(\mathbf{r}). \quad \ldots (1)$$

Heres $s(\mathbf{r})$ is the function approximated, the index $i$ identifies the centers for the RBFs (the domain element nodes in this case), while $\mathbf{r}_i$ is the location of that center. $p(\mathbf{r})$ is an optional polynomial term, of any order, that can be added to ensure certain properties of the interpolation (see Refs 38 and 43). The coefficients $\beta_i$ are found by requiring exact recovery of the function values at the data points.

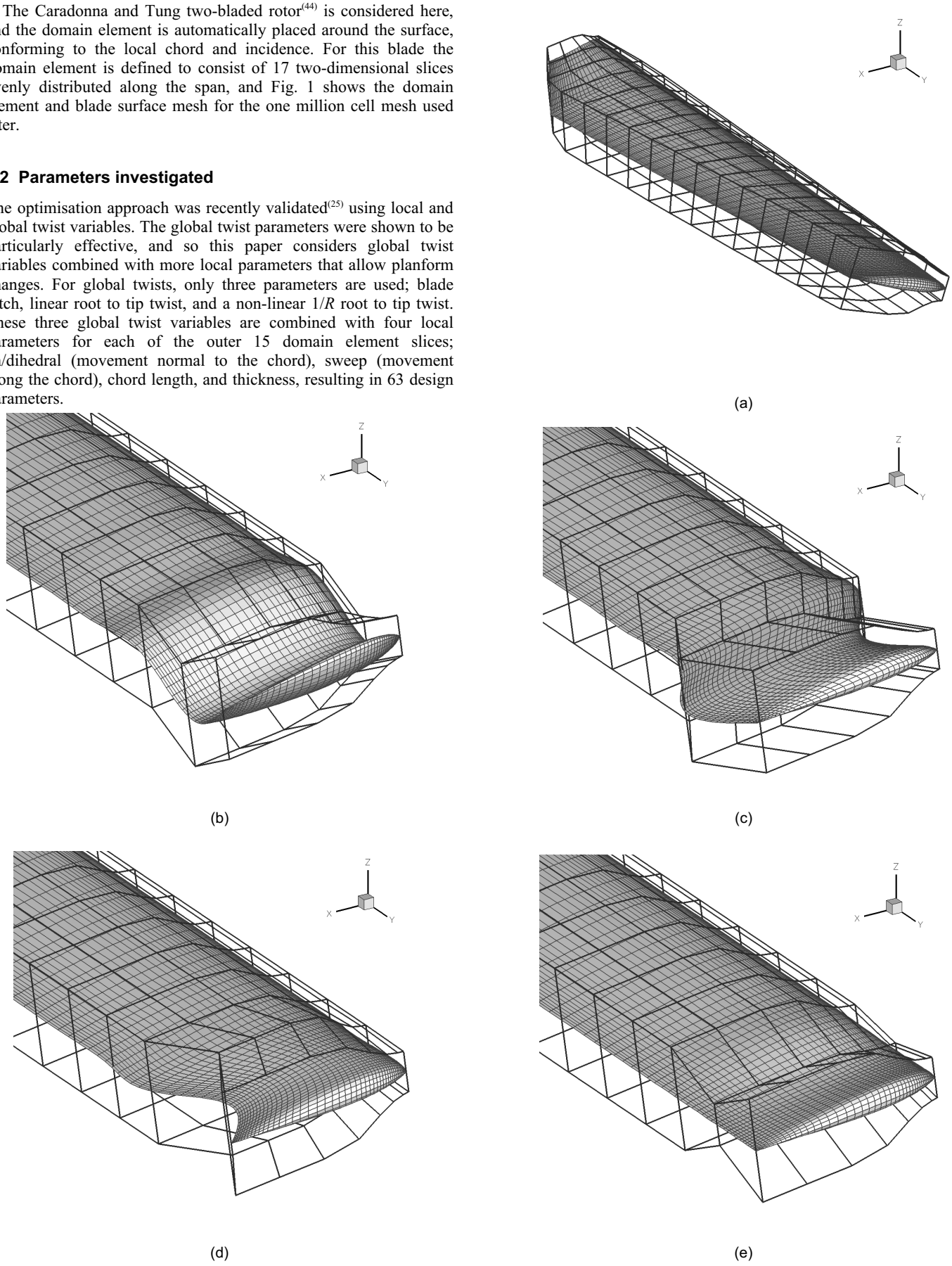
Due to the decaying behaviour of the compact basis functions used here (the $\phi$ values above)[38], the interpolation has a local character, see example later. The exact basis function used and the support radius can be varied to provide smoother or more global changes to both the surface geometry and the volume mesh[38], and the C2 function of Wendland[42] was found to provide the best combination of deformation quality and matrix conditioning, so is used here.

https://doi.org/10.1017/S0001924000006151 Published online by Cambridge University Press

The Caradonna and Tung two-bladed rotor[44] is considered here, and the domain element is automatically placed around the surface, conforming to the local chord and incidence. For this blade the domain element is defined to consist of 17 two-dimensional slices evenly distributed along the span, and Fig. 1 shows the domain element and blade surface mesh for the one million cell mesh used later.

### 2.2 Parameters investigated

The optimisation approach was recently validated[25] using local and global twist variables. The global twist parameters were shown to be particularly effective, and so this paper considers global twist variables combined with more local parameters that allow planform changes. For global twists, only three parameters are used; blade pitch, linear root to tip twist, and a non-linear $1/R$ root to tip twist. These three global twist variables are combined with four local parameters for each of the outer 15 domain element slices; an/dihedral (movement normal to the chord), sweep (movement along the chord), chord length, and thickness, resulting in 63 design parameters.




(a) (b) (c) (d) (e)

Figure 2. Deformed domain element and rotor surface.

https://doi.org/10.1017/S0001924000006151 Published online by Cambridge University Press

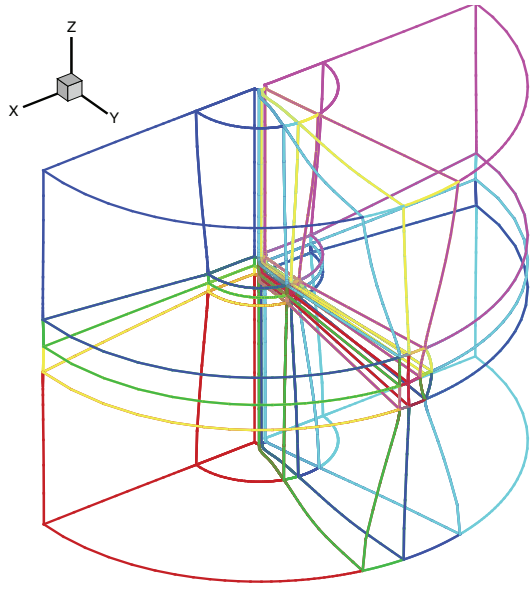



Figure 3. Domain and block boundaries.

Figure 2 shows exaggarated examples of the parameters used. Image (a) shows the deformation for a global linear root to tip twist; the deformed domain element and resulting blade surface are shown. Images (b)-(e) then show a dihedral deformation of the 16th domain element slice, followed by a sweep deformation, chord, and thickness deformations. The flexiblity of the approach and the smoothness of the deformed surface is clear; the volume mesh is deformed in the same smooth fashion, and so no mesh regeneration is required.

### 2.3 Optimisation scheme

The parameterisation and surface and volume mesh deformation approach has been developed such that it is applicable to any mesh type, flow solver, and optimisation scheme. It is linked here to a non-linear Feasible Sequential Quadratic Programming (FSQP)[45,46,47] optimisation algorithm, and this choice is important, since it allows strict enforcement of aerodynamic and geometric constraints. Unconstrained optimisations can incorporate constraints by using a penalty function for design parameters that take the design near or beyond the constraint boundary, but these methods can be inefficient and the method here solves the Kuhn-Tucker equations. The method requires the gradients with respect to each parameter, and has been made independent from the flow-solver by obtaining sensitivity information by finite-differences using a symmetric central-difference stencil, i.e. one positive and one negative perturbation are considered for each design variable. The code is not linked to a flow-solver, but has been written to control its own calls to the solver used, and reads the output back to compute the required gradients.

Since each gradient is computed by separate calls to an external flow-solver, the algorithm has been parallelized such that one parameter (or a group of parameters) is assigned to each available CPU, allowing parallel evaluation of the required sensitivities. Function evaluations and optimiser updates occur on the master process, and each CPU controls the geometry (and CFD volume mesh) perturbation corresponding to a different design variable, and calls the flow solver. Flow-solver results are then returned to the master for optimiser updates.

## 3.0 TWO-BLADED ROTOR AERODYNAMIC OPTIMISATION

A detailed analysis of rotor optimisation using global and local coarse levels of twist only parameters has been presented[25], and proved the effectiveness and robustness of the scheme. Hence, the parameters are extended here to allow more flexibility.

The Caradonna and Tung two-bladed rotor[44] is a rectangular blade, aspect ratio 6, constant NACA0012 section, with no twist or taper. The case chosen was the 8° collective pitch case, and optimisation performed for a transonic tip Mach number, $M_{Tip}$ = 0·877, since this includes the effect of wave drag due to the transonic region. A one million cell structured multiblock mesh was used, generated using the techniques in Ref 48. Fig. 3 shows the domain and block boundaries.

### 3.1 Flow-solver

The flow-solver used is a structured multiblock finite-volume, unsteady, inviscid upwind code[49] using the flux vector splitting of van Leer[50]. Convergence acceleration is achieved through multigrid[12,51]. The method solves the Euler equations in integral form and, for hovering rotor cases, the three-dimensional unsteady

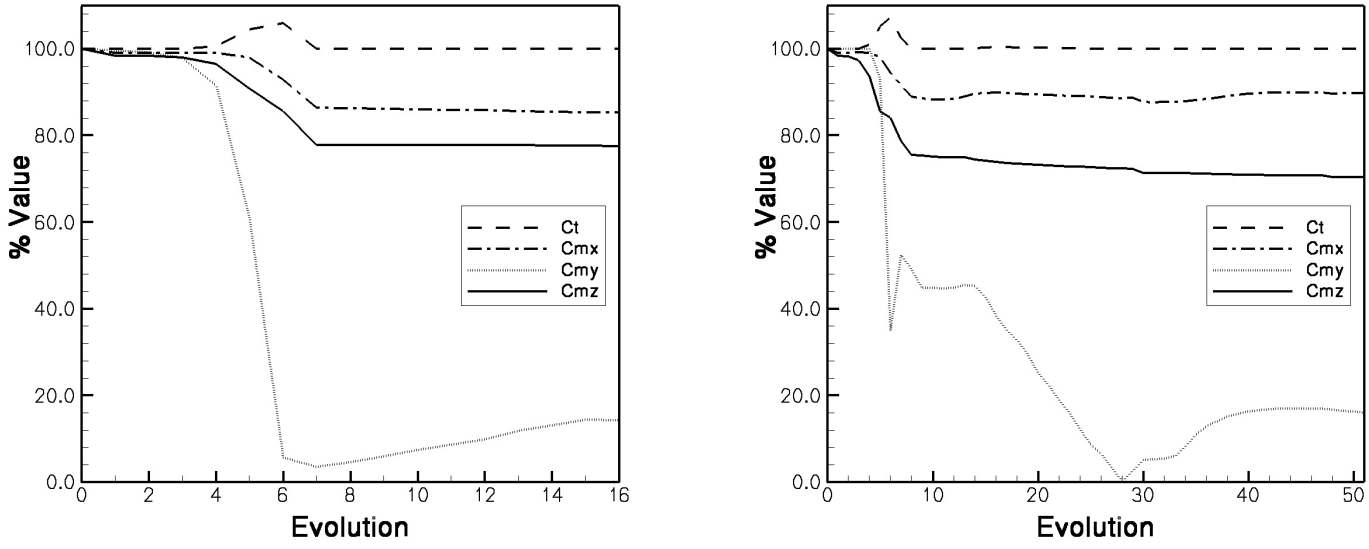



Figure 4. Convergence histories, 3 (left) and 63 (right) parameters.

https://doi.org/10.1017/S0001924000006151 Published online by Cambridge University Press

Euler equations are transformed to a blade-fixed rotating reference frame.

Clearly an inviscid solution will not model skin friction, which is an important component of drag (torque), but the other significant aspects of this design problem, namely minimisation of induced power, wave drag, and blade-vortex interaction, can be performed using an inviscid model. Since the aim of this work is to develop an optimisation framework, independent of the flow-solver, it was deemed acceptable to use an inviscid model to demonstrate the technology.

### 3.2 Optimisation results

The two optimisations were run in parallel on four and 64 CPUs (one per variable plus one for the master process). The cases were run with strict constraints:

| **Objective** | **Minimise $C_Q$ (=$C_{mz}$)** |
|---|---|
| Constraint 1 | $C_T \geq C_T^{orig}$ |
| Constraint 2 | $C_{mx} \leq C_{mx}^{orig}$ |
| Constraint 3 | $\lvert C_{my}\rvert \leq \lvert C_{my}^{orig}\rvert$ |
| Constraint 4 | $V_{int} \geq V_{int}^{orig}$ |

Table 1 shows results of the optimisations, and so both have resulted in a significant reduction in torque. Furthermore, the other two moments have also been reduced, the bending moment by a significant amount.

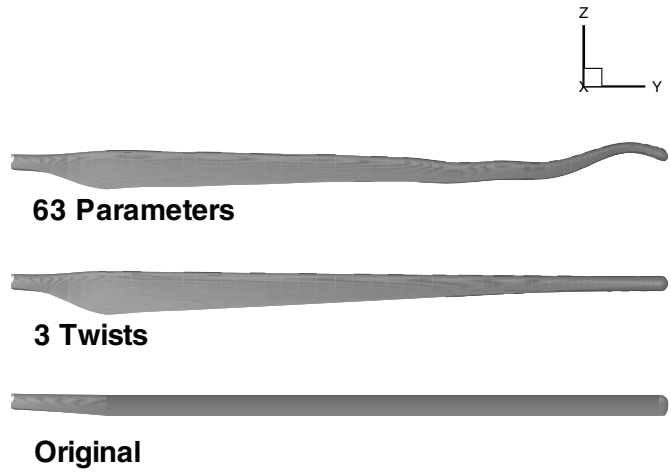
The convergence histories of the two cases are presented in Fig. 4. Hence, the three twist case converges very quickly, with most of the gain achieved in the first seven evolutions. Using only three global twists has resulted in a 22% reduction in torque. A large proportion of the 63 parameter gain is also achieved very quickly, and it is assumed this is due to the twist parameters approaching their final values rapidly since they have significantly larger sensitivities than the local parameters. The remaining reductions are then due to the local parameters, with these allowing a further 7% reduction in torque.

Three views of the original and optimised blades are shown in Figure 5, the lower two views also showing upper and lower surface pressure coefficient contours; 57 evenly-spaced contours are plotted between –1·8 and 1·2. The twist and loading distributions are shown in Figure 6 (here $C_z$ is the sectional normal force coefficient), and so the optimisation has produced significant twist alterations in both cases.

Considering the pressure contours and loading, it is clear that the twist only case has attempted to reduce torque by minimising the induced power, i.e. tending towards as linear a loading as possible, but these parameters have little scope to reduce the wave drag. The 63 parameter case has resulted in significant geometric changes, with twist, sweep, dihedral and thickness changes. In fact this has resulted in almost a halving of the section thickness in the transonic region, along with an 18% increase in chord and 29% forward movement of the quarter chord position. Hence, this approach is extremely flexible, with significant planform changes possible. The

**Table 1**
**Optimisation results**

| Parameters | 3 | 63 |
|---|---|---|
| Evolutions | 16 | 51 |
| | % Differences | |
| $C_T$ | 0·0 | 0·0 |
| $C_{mx}$ | –14·8 | –10·3 |
| $C_{my}$ | –86·6 | –84·0 |
| Volume | 0·0 | 0·0 |
| $C_{mz}$ | –22·5 | –29·6 |



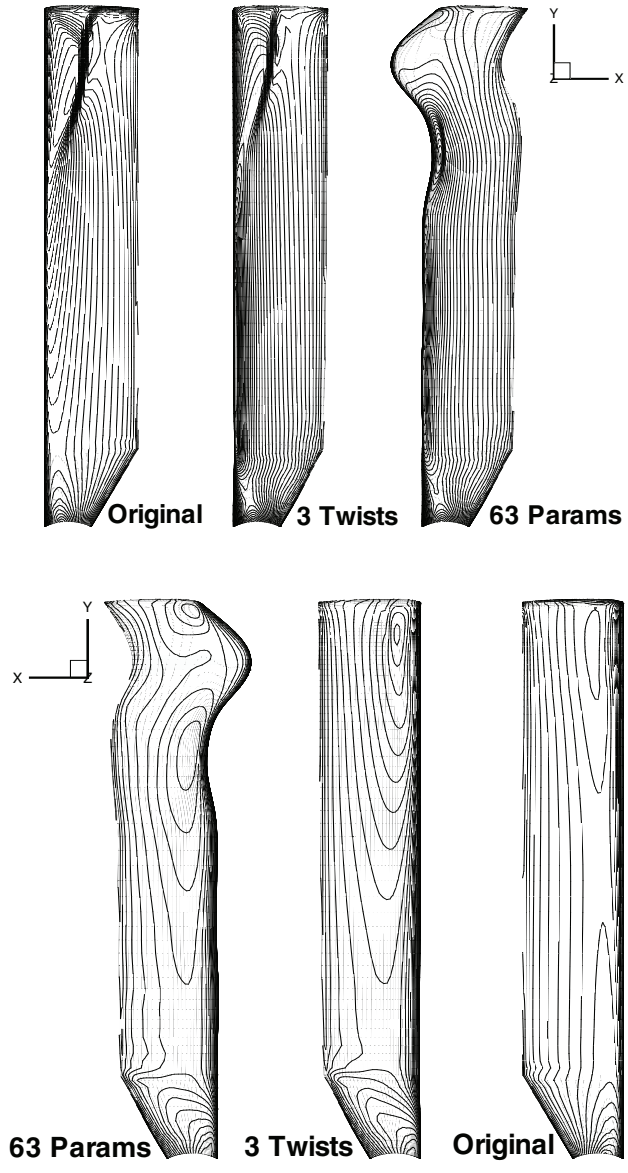




Figure 5: Original and optimised surfaces and pressure coefficient contours.

https://doi.org/10.1017/S0001924000006151 Published online by Cambridge University Press

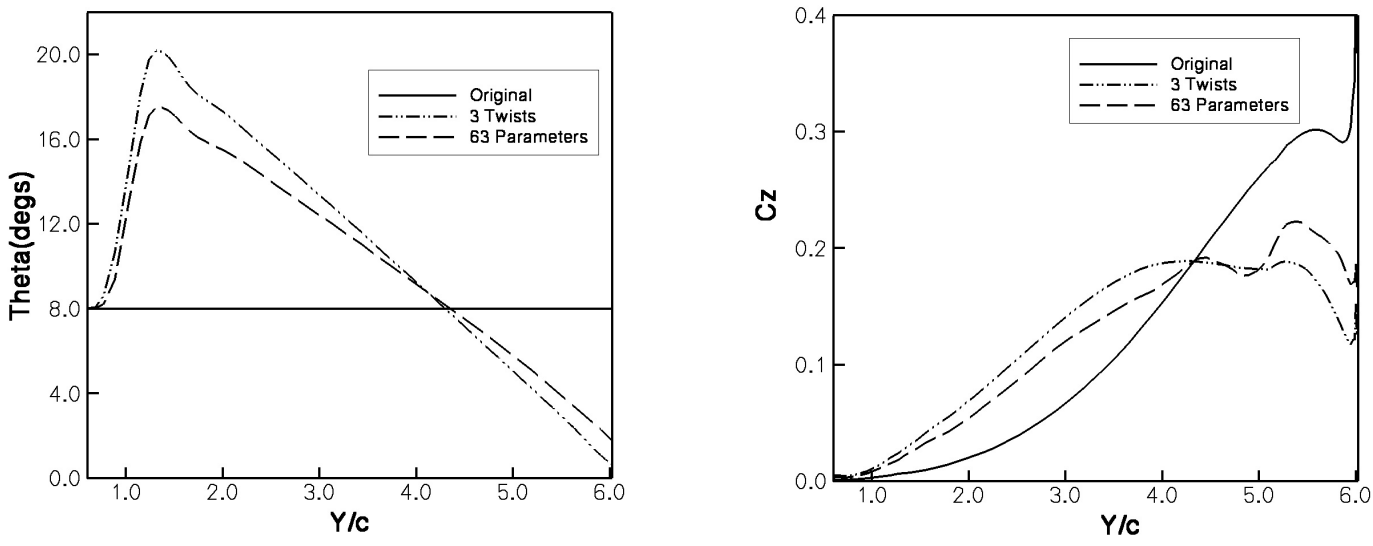



Figure 6. Original and optimised twist and loading distributions.

reduction of the transonic region also results in a large reduction in bending moment ($C_{my}$). Clearly the majority of the local changes are in the transonic region where the sensitivities are large due to the wave drag, and so this case has attempted to minimise both the induced power and wave drag. Furthermore, there is also di/anhedral in the tip region in this case, in an attempt to reduce the blade-vortex interaction. It is very interesting to note that the optimised blade shape has deformed towards the AgustaWestland BERP blade, see for example[52,53], which was designed using lower fidelity methods, and was also designed for forward flight performance.

It is also important to consider off-design performance, so complete thrust-torque polars were computed for the original blade, and the two optimised blades, and these are presented in Figure 7; quarter degree increments in collective pitch were used over the entire range. Hence, the blade optimised using 63 parameters has a performance advantage over the original blade at all positive thrust values above a small value, and also performs very closely at negative thrust. The twist only case also performs better than the original blade for all positive thrusts above a slightly higher value. It also exhibits an almost constant offset from the 63 parameter case. The performance at negative and low positive thrust is worst than the original blade due to the increased transonic flow on the lower surface of the twisted blade.

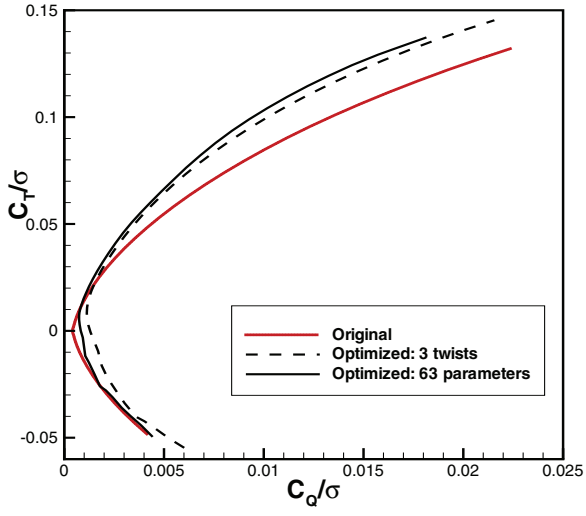



Figure 7. Performance polars, original and optimised blades.

## 4.0 CONCLUSIONS

A generic and efficient domain element method of geometric parameterisation has been presented for application to CFD-based aerodynamic optimisation. Design surface control and volume mesh deformation are the key issues when considering optimisation, and both are solved using this approach. A radial basis function global interpolation allows the domain element to control the grid coordinates and provide simultaneous deformation of the design surface and its corresponding CFD mesh. This approach is totally independent of mesh type, so requires no connectivity, and both the design surface and volume meshes are deformed in a smooth, high quality fashion, regardless of the size of the deformation.

The surface parameterisation and mesh deformation scheme has been linked to an advanced feasible sequential quadratic programming (FSQP) gradient-based optimiser, and this has been parallelized, such that optimisation of the rotor can be performed in a practical run time. The optimisation suite has been parallelised in a generic fashion such that the code is still independent of the flow solver.

To demonstrate the optimisation framework an inviscid flow-solver has been used for initial tests. Results have been presented for a twist only optimisation, and an optimisation where the parameters have been extended to allow global and local planform geometric changes, for a transonic tip speed case. Torque reductions of 22% have been achieved using only three global twists, and this also requires very few evolutions to converge. Using these three twist parameters plus 60 local parameters allows a further 7% torque reduction, and these results are very impressive. Large geometric changes have been demonstrated, due to the optimiser attempting to reduce the induced power, the wave drag, and blade-vortex interaction effects, showing the effectiveness and flexibility of the scheme. Off-design performance has also been improved, for both optimised blades, at all positive thrust values above a low value.

## ACKNOWLEDGEMENTS

The authors would like to thank Dr Asa Morris for his contribution to the development of the parallel optimiser.

## REFERENCES

1. LI, W. HUYSE L. and PADULA, S. Profile Optimisation Method for Robust Aerofoil Shape Optimisation in Viscous Flows NASA/TM-2003-212408.

https://doi.org/10.1017/S0001924000006151 Published online by Cambridge University Press

NASA/CR-2001-211042. icase report no 2001-22.
2. HICKS, R.M., MURMAN, E.M. and VANDERPLAATS, G.N. An Assessment of Aerofoil Design by Numerical Optimisation NASA TMX-3092, Ames Research Center, Moffett Field, California, USA, July 1974.
3. HICKS, R.M. and HENNE, P.A. Wing design by numerical optimization, *J Aircr*, 1978, **15**, pp 407-412.
4. REUTHER, J., JAMESON, A., FARMER, J., MARTINELLI, L. and SAUNDERS, D. Aerodynamic Shape Optimization of Complex Aircraft Configurations via an Adjoint Formulation RIACS Technical Report 96.02 January 1996. Presented at the AIAA 34th Aerospace Sciences Meeting and Exhibit, January 1996, AIAA paper 96-0094.
5. CHUNG, H.S. and ALONSO, J. Multiobjective optimization using approximation model-based genetic algorithms AIAA 2004-4325 10th AIAA/ISSMO Symposium on Multidisciplinary Analysis and Optimization 30 August – 1 September, 2004/Albany, New York, USA.
6. GUMBERT, C.R., HOU, G. and NEWMAN, P.A. Simultaneous Aerodynamic Analysis and Design Optimization (SAADO. for a 3D Rigid Wing AIAA 99-3296).
7. WONG, W.S., LE MOIGNE, A. and QIN, N. Parallel adjoint-based optimisation of a blended wing body aircraft with shock control bumps, *Aeronaut J*, March 2007, **111**, (1117), pp 165-174.
8. GUMBERT, C.R., HOU, G. and NEWMAN, P.A. Simultaneous Aerodynamic Analysis and Design Optimization (SAADO) for a 3D Flexible Wing AIAA 2001-1107.
9. JAMESON, A., LEOVIRIYAKIT, K. and SHANKARAN, S. Multi-point aero-structural optimization of wings including variations, 45th AIAA Aerospace Sciences Meeting and Exhibit, Reno, USA, January 2007.
10. ALLEN, C.B. Parallel simulation of unsteady hovering rotor wakes, *Int J Numerical Methods in Engineering*, 2006, **68**, (6), pp 632-649.
11. ALLEN, C.B. Convergence of steady and unsteady formulations for inviscid hovering rotor solutions, *Int J Numerical Methods in Fluids*, 2003, **41**, (9), pp 931-949.
12. ALLEN, C.B. An unsteady multiblock multigrid scheme for lifting forward flight rotor simulation, *Int J Numerical Methods in Fluids*, 2004, **45**, (9), pp 973-984 (DOI 10.2/fld.711).
13. CELI, R. Recent applications of design optimisation to rotorcraft – A survey, *J Aircr,* 1999, **36**, (1).
14. LE PAPE, A. and BEAUMIER, P. Numerical optimisation of helicopter rotor aerodynamic performance in hover, *Aerospace Science and Technology*, 2005, **9**, pp 191-201.
15. DUMONT, A., LE PAPE, A., PETER, J. and HUBERSON, S. Aerodynamic shape optimisation of hovering rotors using a discrete adjoint of the RANS equations, Presented at AHS 65th Annual Forum, Grapevine, TX, May 2009.
16. NADARAJAH, S. and TATOSSIAN, C. Adjoint-based aerodynamic shape optimsation of rotorcraft blades, AIAA-2008-0322, 26th AIAA Applied Aerodynamics Conference, Hawaii, USA, August 2008.
17. CHOI, S., POTTSDAM, M., LEE, K.H., IACCARINO, G. and ALONSO, J.J. Helicopter rotor design using a time-spectral and adjoint-based method, AIAA 2008-5810, 12th AIAA/ISSMO Multidisciplinary Analysis and Optimisation Conference, 2008, Victoria, BC, Canada.
18. NIELSEN, E.J., LEE-RAUSCH, E.M. and JONES, W.T. Adjoint-based design of rotors using the navier-stokes equations in a noninertial frame, Presented at AHS 65th Annual Forum, Grapevine, TX, May 2009.
19. IMIELA, M. High-fidelity optimization framework for helicopter rotors, proceedings 25th European Rotorcraft Forum, Hamburg, Germany, 2009.
20. IMIELA, M. Investigation of aeroelastic effects for a helicopter main rotor in hover, proceedings 26th European Rotorcraft Forum, Paris, France, 2010.
21. JOHNSON, C.S. and BARAKOS, G.N. Optimising aspects of rotor blades in forward flight, AIAA paper 2011-1194, Proceedings 49th AIAA Aerospace Sciences Meeting including the New Horizons Forumand Aerospace Exposition, Orlando, Florida, USA, 4-7 January 2011.
22. JOHNSON, C.S. and BARAKOS, G.N. A framework for optimising aspects of rotor blades, *Aeronaut J*, March 2011, **115**, (1163), pp 147-161.
23. MORRIS, A.M., ALLEN, C.B. and RENDALL, T.C.S. CFD-based optimization of aerofoils using radial basis functions for domain element parameterization and mesh deformation, *Int J Numerical Methods in Fluids*, 2008, **58**, (8), pp 827-860.
24. MORRIS, A.M., ALLEN, C.B. and RENDALL, T.C.S. Domain-element method for aerodynamic shape optimization applied to modern transport wing, *AIAA J*, 2009, **47**, (7), pp 1647-1659.
25. ALLEN, C.B., RENDALL, T.C.S. and MORRIS, A.M. Computational-fluid-dynamics-based twist optimization of hovering rotors, *J Aircr*, **47**, (6), 2010, pp 2075-2085.
26. JAMESON, A. Aerodynamic design via control theory, *J Sci Comput*, 1988, **3**, pp 233-260.
27. REUTHER, J Aerodynamic Shape Optimisation Using Control Theory, NASA Technical report NASA-CR-201064, 1996.
28. JAMESON, A. Automatic Design of Transonic Aerofoils to Reduce the Shock Induced Pressure Drag In Proceedings of the 31st Israel Annual Conference on Aviation and Aeronautics, Tel Aviv, Israel, pp 5-17, February 1990.
29. PICKETT, R.M., RUBINSTEIN, M.F. and NELSON, R.B. Automated structural synthesis using a reduced number of design coordinates, *AIAA J*, 1973, **11**, (4), pp 494-498.
30. WATT, A. and WATT, M. *Advanced Animation and Rendering Techniques*, Addison-Wesley, New York, USA, 1992, Chapter 17.
31. http://www.optimalsolutions.us/
32. ANDERSON, W.K., KARMAN, S.L. and BURDYSHAW, C. Geometry parameterisation method for multidisciplinary applications, *AIAA J*, 2009, **17**, (6), pp 1568-1578.
33. BLOOR, M.I.G. and WILSON, M.J. Efficient parameterisation of generic aircraft geometry, *J Aircr*, 1995, **32**, (6), pp 1269-1275.
34. BRAIBANT, V. and FLEURY, C. Shape optimal design using B-splines, *Computer Methods in Applied Mechanics and Engineering*, August 1984, **44**, (3), pp 247-267.
35. KULFAN, B.M. A universal parametric geometry representation method – CST 45th AIAA Aerospace Sciences Meeting and Exibit 8-11 January 2007, Reno, Nevada, USA.
36. SAMAREH J.A. Survey of shape parameterisation techniques for high-fidelity multidisciplinary shape optimisation, *AIAA J*, May 2001, **39**, (5), pp 877-884.
37. NADARAJAH, S., CASTONGUAY, P. and MOUSAVI, A. Survey of shape parameterization techniques and its effect on three-dimensional aerodynamic shape optimisation, AIAA-2007-3837,18th AIAA Computational Fluid Dynamics Conference, Miami, FL, USA, 25-28 June 2007.
38. RENDALL, T.C.S. and ALLEN, C.B. Unified fluid-structure interpolation and mesh motion using radial basis functions, *Int J Numerical Methods in Engineering*, 2008, **74**, (10), pp 1519-1559.
39. RENDALL, T.C.S. and ALLEN, C.B. Efficient mesh motion using radial basis functions with data reduction algorithms, *J Computational Physics*, **228**, (17), 2009, pp 6231-6249.
40. RENDALL, T.C.S. and ALLEN, C.B. Parallel efficient mesh motion using radial basis functions with application to multi-bladed rotors, *Int J Numerical Methods in Engineering*, 2010, **81**, (1), pp 89-105.
41. BUHMANN, H. *Radial Basis Functions*, Cambridge University Press, 1st ed, 2005.
42. WENDLAND, H. *Scattered Data Approximation*, Cambridge University Press, 1st ed, 2005.
43. MACKMAN, T.J. and ALLEN, C.B. Investigation of an adaptive sampling method for data interpolation using radial basis functions, *Int J for Num Methods in Engineering*, 2010, **83**, (7), pp 915-938.
44. CARADONNA, F.X. and TUNG, C. Experimental and analytical studies of a model helicopter rotor in hover, NASA TM-81232, September 1981.
45. ZHOU, J.L., TITS, A.L. and LAWRENCE, C.T. User's Guide for FFSQP Version 3.7: A Fortran Code for Solving Optimisation Programs, Possibly Minimax, with General Inequality Constraints and Linear Equality Constraints, Generating Feasible Iterates, Institute for Systems Research, University of Maryland, Technical Report SRC-TR-92-107r5, College Park, 1997.
46. ZHOU, J.L. and TITS, A.L. Nonmonotone line search for minimax problems, *J Optimisation Theory and Applications*, 1993, **76**, (3), pp 455-476.
47. PANIER, E. and TITS, A.L. On combining feasibility, descent and superlinear convergence in inequality constrained optimisation, *Mathematical Programming*, 1993, **59**, pp 261-276.
48. ALLEN, C.B. Towards automatic structured multiblock mesh generation using improved transfinite interpolation, *Int J Numerical Methods in Engineering*, 2008, **74**, (5), pp 697-733.
49. ALLEN, C.B. Parallel universal approach to mesh motion and application to rotors in forward flight, *Int J Numerical Methods in Engineering*, 2007, **69**, (10), pp 2126-2149.
50. PARPIA, I.H. Van-Leer flux vector splitting in moving co-ordinates, *AIAA J*, 1988, **26**, pp 113-115.
51. ALLEN, C.B. Multigrid acceleration of an upwind euler code for hovering rotor flows, *Aeronaut J*, September 2001, **105**, (1051), pp 517-524.
52. PERRY, F.J. Aerodynamics of the helicopter worldspeed record, Presented at the 43rd Annual National Forum of the American Helicopter Society, May 1987.
53. ISAACS, N.C.G. and HARRISON, R.J. Investigation of retreating blade stall mechanisms using flight test pressure measurements, Presented at the 45th Annual National Forum of the American Helicopter Society, May 1989.

https://doi.org/10.1017/S0001924000006151 Published online by Cambridge University Press